AMCBRIDGE
Tel: +1 866-575-4791
Fax: +1 973-895-5376
E-mail: contact@amcbridge.com

Surface Reconstruction Based on Neural Network

1. Introduction

"Machine learning is the science of getting computers to act without being explicitly programmed. In the past decade, machine learning has given us self-driving cars, practical speech recognition, effective web search, and a vastly improved understanding of the human genome." [1]

Surface reconstruction is an important trend in 3D scanning. The problem is to recreate surfaces from a given point cloud within the shortest possible time and with a given quality criteria. There is a set of different approaches for solving this problem, which includes Self-Organized Maps [2], Bayesian reconstruction [3] and Poisson reconstruction [4].

The aim of the research is to find the most suitable method based on Machine Learning unsupervised learning techniques for reconstruction of interior and exterior 3D scans of original objects. The self-organizing map (SOM) [5] type of the artificial neural network (ANN) was chosen, due to its ability to produce good results without restrictions on point cloud size and points' order. It can generate meshes from a small number of point samples in an unorganized point cloud.

The purpose of this article is to analyze and compare results obtained with the usage of two self-organizing map types – Surface Growing Neural Gas [6] and Growing Cell Structures reconstruction [7] – for reconstruction of a 3D mesh from point cloud. In addition, the sGNG extension to multithreading is presented and compared to the original approach.

2. Terminology

A point cloud is a set (organized or unorganized) of points in space, it represents a certain mesh and is located in some coordinate system.

A polygon mesh is a collection of vertices (points), edges (connections between vertices) and faces (e.g. triangles) that defines the shape of the object. [8]

ANN is "a computing system made up of a number of simple, highly interconnected processing elements, which process information by their dynamic state response to external inputs" [9].

SOM implements an orderly mapping of a high-dimensional distribution onto a regular low-dimensional grid. [5]

Tel: +1 866-575-4791
Fax: +1 973-895-5376
E-mail: contact@amcbridge.com

GNG is a SOM, where new units are added successively "to an initially small network by evaluating local statistical measures gathered during previous adaptation steps". [10]

GCS is a SOM based on creation of consistent mesh structure by approximation of vertices positions to the point sample coordinates, edge split and vertex collapse. [11]

Valence of the vertex is the number of edges connecting other vertices to the given one.

Mesh with the appropriate *quality* is defined as the 2-manifold mesh that is smooth, consistent and has no or few unexpected triangles and holes.

Box is the part of the point cloud that is used by a reconstruction instance in the multithreading approach.

3. Analytics

3.1. Method Description

Surface Growing Neural Gas (sGNG) [6] is a reconstruction algorithm based on GNG with a large number of improvements. Our implementation is based on FGNG [12], which is written in C++, works fast and has a convenient API. It has been modified according to [6] and the results are post-processed for removing unexpected holes. The most important changes are: the process of activity update, triangle creation and triangle flip, additional triangle creation and modified edge split. Activity of the best matching vertex allows to detect regions where vertex density is lower than the density of the input points. Updating activity of vertex has been modified. Instead of incrementing activity values for each vertex in the list on every iteration, it has been decided to store iteration number of last activity for each vertex. The main idea is to compare current iteration number with vertex last activity iteration number, and remove it if it doesn't satisfy condition. This changes the complexity of the algorithm updating vertices activity from O(N) to O(1). Complexity of vertex removal stays the same, according to [6]. Triangle creation, triangle flip and additional triangle creation have been added to the algorithm to improve the smoothness of the surface and prevent the occurrence of non-2-manifold edges. Edge splitting has been modified by performing the split in the middle of the longest edge, instead of the middle of the edge connected with its most active neighbor.

Reconstruction algorithm based on GCS [13] is modified by replacing edge split and vertex removal with vertex split and edge collapse, as the last ones work better in 3D space. Also, adjusting vertex position by linear combination with a sample and Laplacian tangential neighbor smoothing improve the quality of the mesh and prevent the surface from stacking to a local minimum or folding over.

Tel: +1 866-575-4791
Fax: +1 973-895-5376
E-mail: contact@amcbridge.com

The parallel computation of the nearest neighbor was added to both algorithms, to improve the speed for the huge number of vertices.

3.2. Mesh Quality Metrics

A set of metrics was used for reconstructed models for quality measurement.

Runtime Performance shows the suitability of each method for the online reconstruction, especially on the huge point clouds.

Mean Valence [6] shows whether the connections between vertices are distributed uniformly, for smoothness of the mesh. It is calculated as the average of the number of the direct topological neighbors of each vertex in the reconstructed mesh. The ideal vertex valence lies in the range from 4 to 7.

Valences 4-7 metric represents the ratio of the number of the vertices with the most suitable valences in the range from 4 to 7 to the number of all vertices.

Mean Regularity [6] and Mean Aspect [14] ratio represent the mean quality of the triangles, which is defined as the closeness of a given triangle to an equilateral one, from different perspectives. The closer is the triangle to an equilateral, the greater the regularity and the lower the aspect.

Mean Regularity is calculated as the average regularities of the mesh elements (in our case – triangles). The regularity of the element is the ratio between the smallest distance and the largest distance of its vertices to its barycenter.

Aspect ratio of a triangle is the ratio of its largest edge to its smallest one.

Mean Stretch ratio shows the grain of the mesh due to the fact that the stretch ratio of a triangle depends on its size, allowing us to identify the bad triangles with long edges. Stretch ratio is based on the radius of the incircle of the element and length of its longest edge.

3.3. Self-Organizing Neural Network Bottlenecks and Its Solution

The main bottleneck of the neural networks of this type is the Nearest Neighbor Search that is performed at each iteration. Various approaches were introduced to perform this operation faster.

The basic approach is to iterate over all nodes at the current neural network state and compute their distances to the input sample. This algorithm introduces O(N) complexity at each iteration. Although the algorithm could be boosted by CUDA [15], the data transfers required for node deletion and mesh improvement techniques (triangle flip, edge flip, etc.) at each iteration make the CUDA-based NN Search even slower than the CPU-based one.

Tel: +1 866-575-4791
Fax: +1 973-895-5376
E-mail: contact@amcbridge.com

Another NN Search approach – R-Tree, proposed by [16], introduces better complexity O(log N). The use of this sparse tree data structure provides significant improvement in NN Search according to the tests. The disadvantage of R-Tree is the complex structure, making the task of implementation on the GPU challenging. Although the GPU-based R-Tree approaches exist, they outperform the CPU-based one only at datasets larger than 1,000,000 points.

The main issue of the approaches mentioned above is their dependency on the number of nodes. This problem was partially solved in Growing Uniform Grid Structure [17]. The NN Search query complexity is close to constant with the O(N) complexity in the worst case. Although it requires O(N) for growth, the number of growth phases decreases significantly during the increase of nodes. Due to the fact that the NN search query examines very small amount of points, addition of the CUDA improvements is useless.

3.4. Reconstruction Results Analytics

A set of representative reconstruction samples is demonstrated below. The models were taken from the Stanford 3D Scanning Repository and Artec3D scanned models. All the pictures below are obtained with the usage of Point Cloud Library [18] and Visualization Toolkit [19]. All charts were created using Python Matplotlib [20].

In addition, Runtime Performance was compared to standard PCL Poisson reconstruction algorithm. The number of vertices in each case is equal to 10,000.

Model: Stanford Bunny

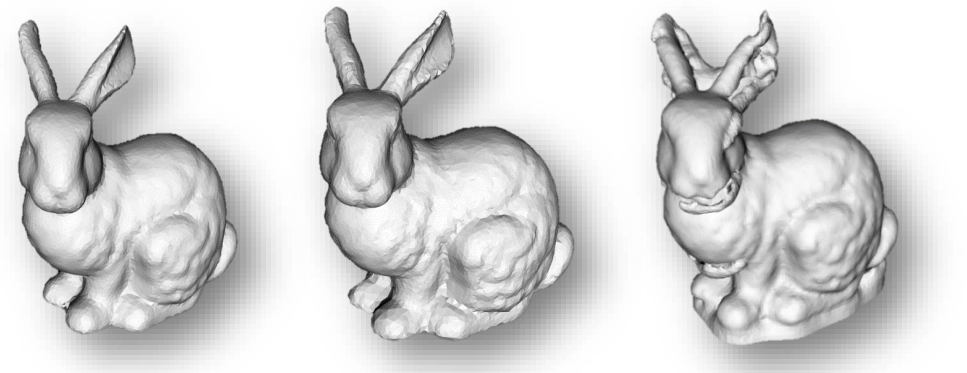

Figure 1. sGNG (left) reconstructed a more consistent surface than GCS (middle) and, especially, PCL Poisson algorithm (right).

Tel: +1 866-575-4791
Fax: +1 973-895-5376
E-mail: contact@amcbridge.com

The sGNG approach provides better results than GCS and PCL. There are no unexpected triangles and holes, the surface is smooth and consistent. This approach deals well with the close elements like bunny ears (Figure 2) that are difficult for reconstruction. Both algorithms (sGNG and GCS) reconstruct smooth target surface with the appropriate quality (Figure 4). In addition, sGNG algorithm is able to process holes that exist in the target mesh (Figure 3). GCS, as expected, produces a less smooth surface, due to the absence of post-processing.

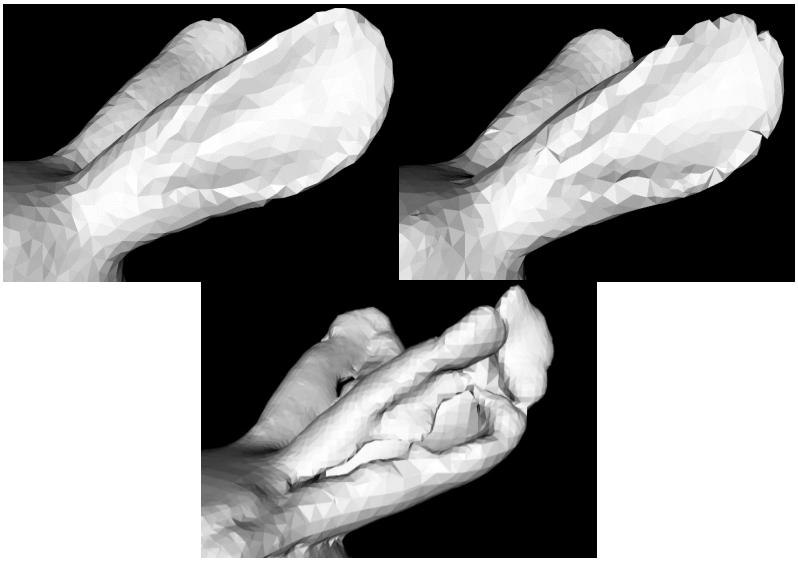

Figure 2. sGNG (top left) reconstructed ears' surface better than GCS (top right) and, especially, PCL Poisson algorithm (bottom).

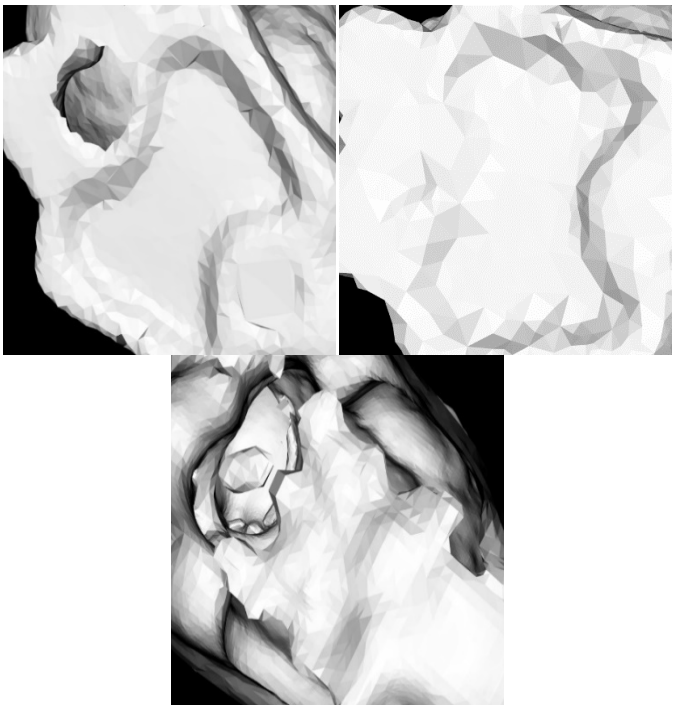

Figure 3. Holes, reconstructed by sGNG (left), do not break the smoothness of the rest surface. GCS (right) is not able to process such holes.

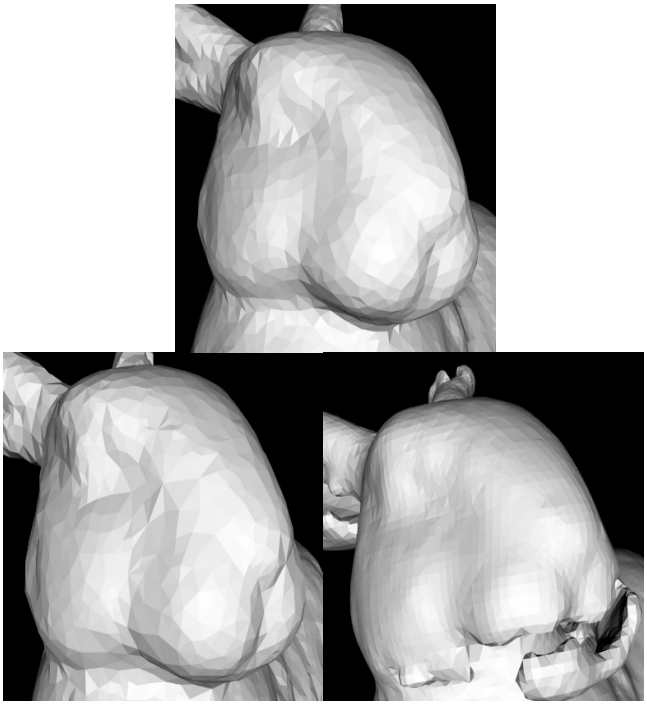

Figure 4. sGNG (top) and GCS (bottom left) reconstructed the bunny face well enough. PCL Poisson algorithm (bottom) has lots of reconstruction errors.

Tel: +1 866-575-4791
Fax: +1 973-895-5376
E-mail: contact@amcbridge.com

Statistics:

As we can see (Figure 5), the performance of sGNG is close to that of PCL, but this algorithm produces a much better result. The GCS algorithm works slower than sGNG algorithm.

The smaller number of the clusters of close vertices at sGNG reconstruction, which can be seen in Figure 3, is explained with the higher Mean Valence and the Valences 4-7 metrics values (Figure 7).

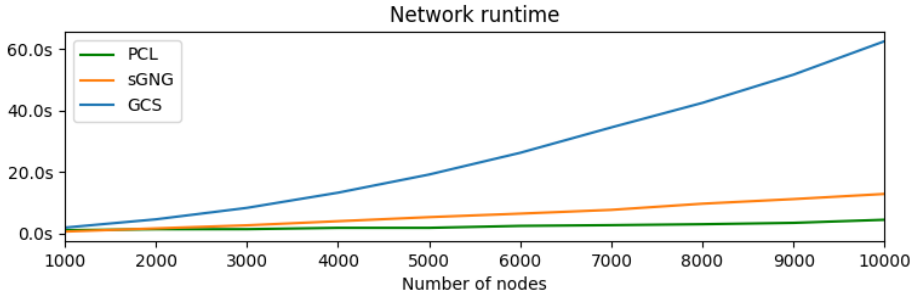

Figure 5.

The performance test of reconstruction algorithms on Stanford Bunny model.

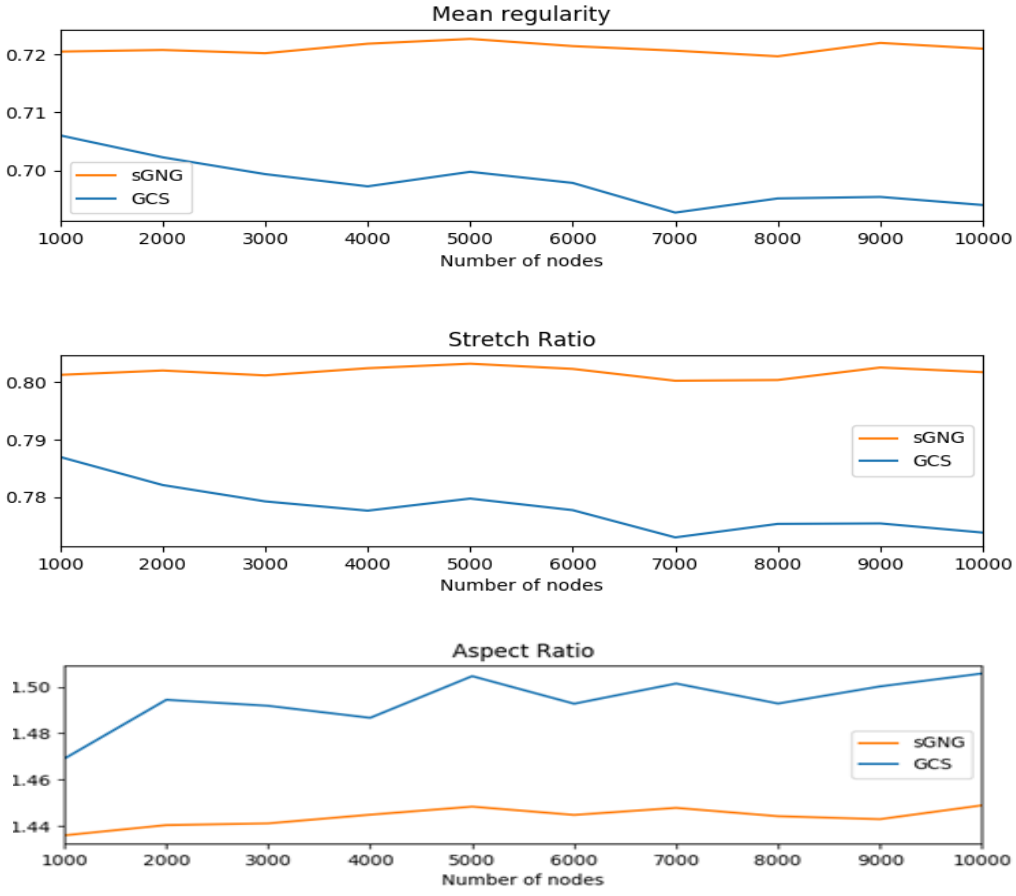

Figure 6. The mean regularity, aspect and stretch ratio metrics for algorithms on Stanford Bunny model.

Tel: +1 866-575-4791
Fax: +1 973-895-5376
E-mail: contact@amcbridge.com

The plots show (Figures 6, 7) that the other metrics are generally the same for both algorithms, which means that the vertex connection distribution and the number of triangles that are close enough to equilateral are nearly the same.

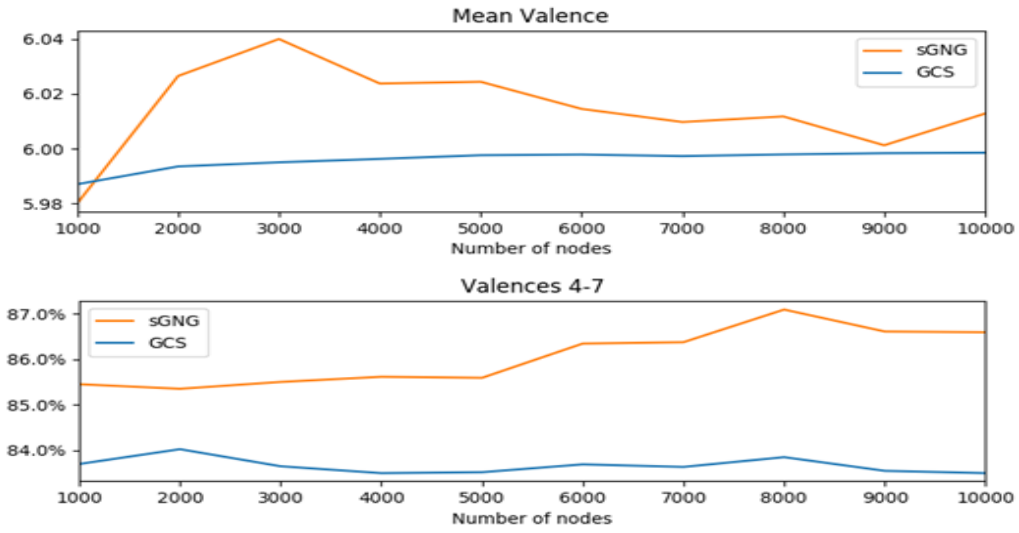

Figure 7. The mean valence and valences 4-7 metrics for algorithms on Stanford Bunny model.

Further testing on the rest of presented models shows results similar to the Stanford Bunny model, so we just make a few important points concerning these models.

Model: Gear

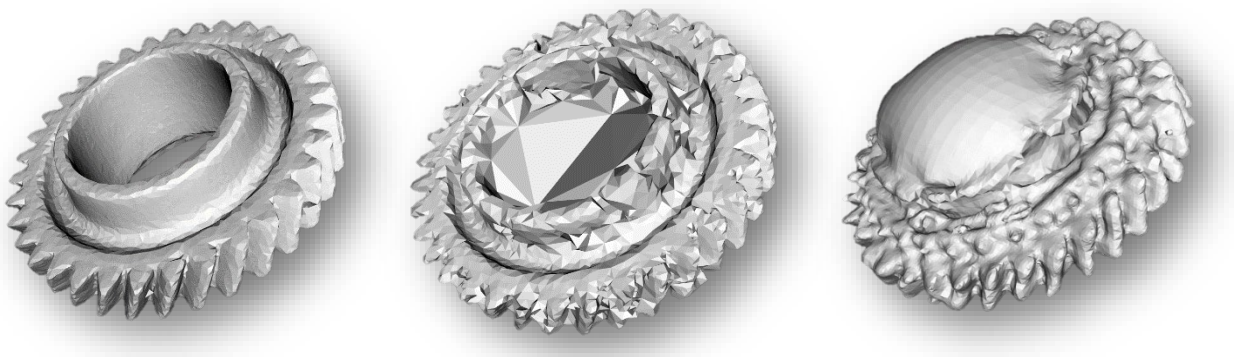

Figure 8. sGNG (left) reconstructed the center hole and the teeth of the gear very well, GCS (middle) showed worse results in reconstruction of the hole due to the specifics of the algorithm. PCL Poisson reconstruction (right) is significantly worse.

Tel: +1 866-575-4791
Fax: +1 973-895-5376
E-mail: contact@amcbridge.com

The results of reconstruction of this model are noticeably different. The sGNG approach reconstructed a very good mesh without any observable errors. GCS partially paved the hole due to the feature of vertex distribution in the reconstructed mesh [21]. Such situations could be handled by post-processing. PCL Poisson completely paved the hole with lots of unexpected elements.

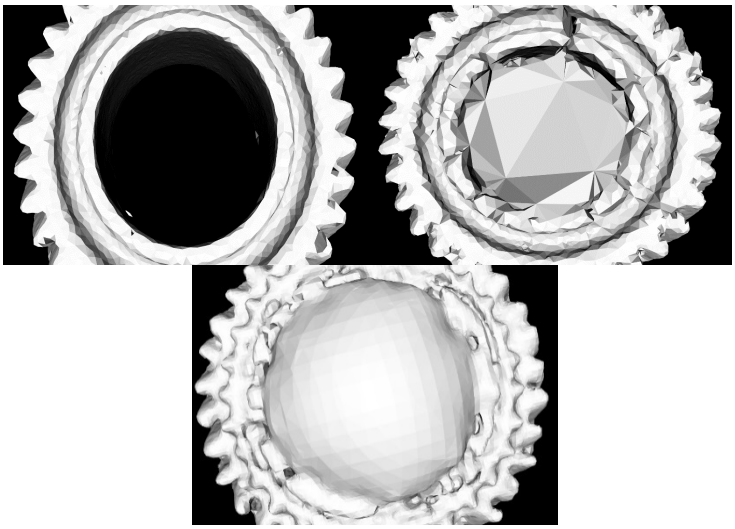

Figure 9. Comparison of the central hole of the gear, reconstructed with sGNG (top left), GCS (top right) and PCL Poisson algorithm (bottom).

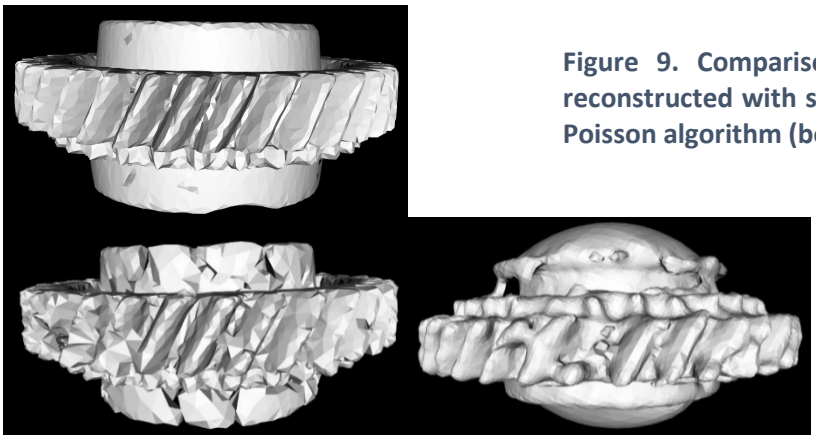

Figure 10. Comparison of the gear`s teeth, reconstructed with sGNG (top), GCS (bottom left) and PCL Poisson algorithm (bottom right).

Statistics:

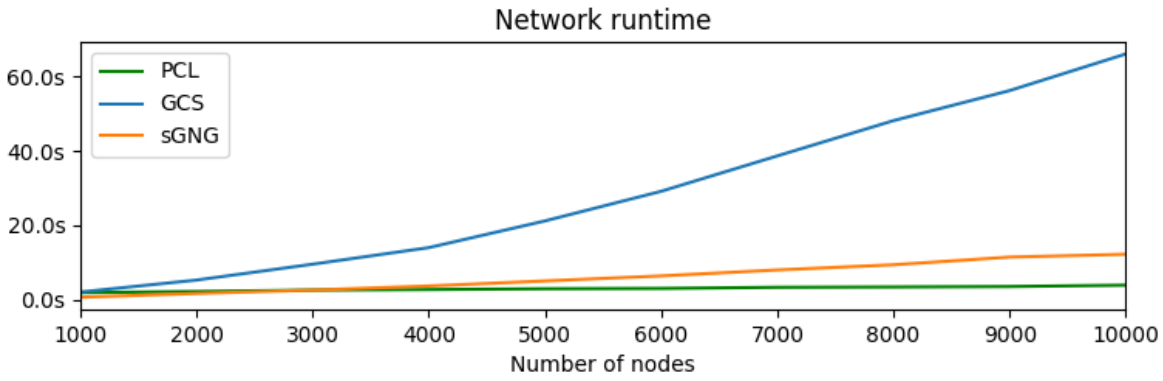

Figure 11. The performance test of reconstruction algorithms on the Gear model.

Tel: +1 866-575-4791
Fax: +1 973-895-5376
E-mail: contact@amcbridge.com

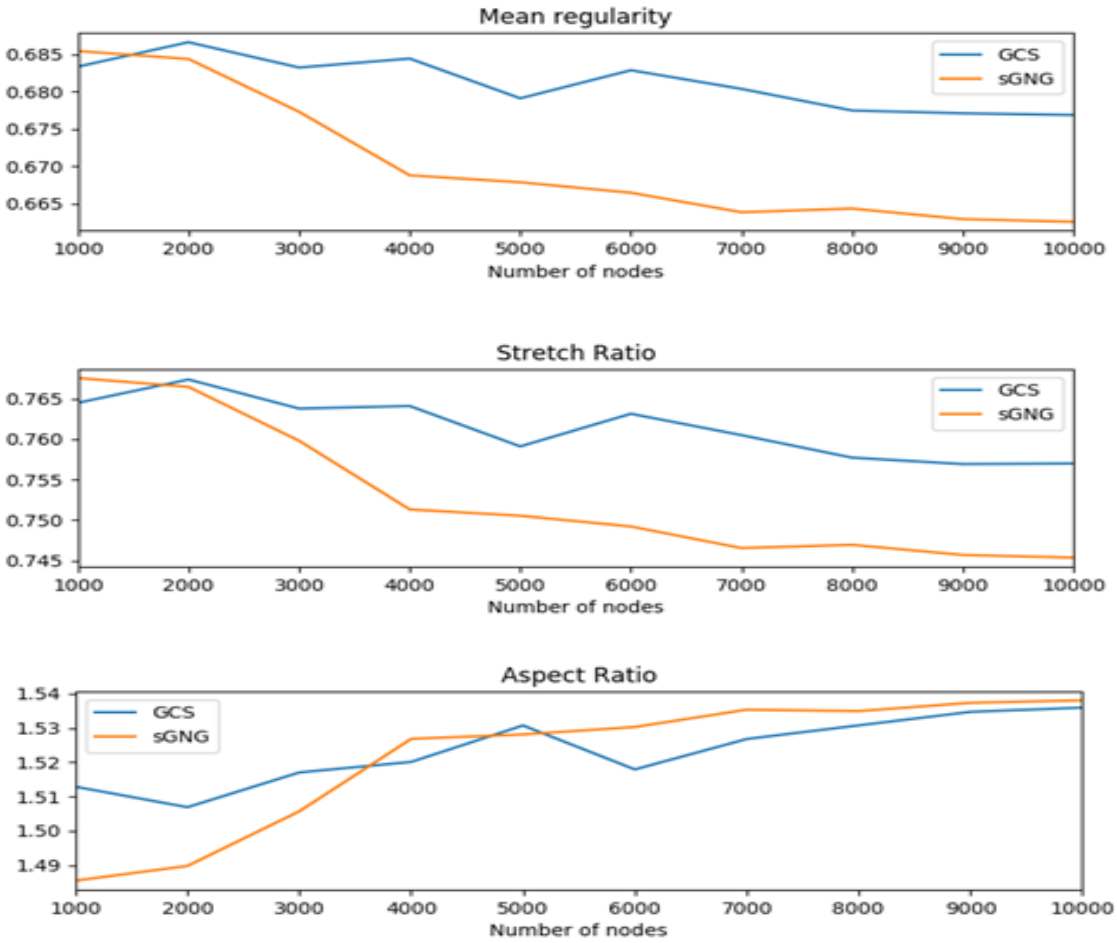

Figure 12. The mean regularity, aspect and stretch ration metrics for algorithms on the Gear model.

Tel: +1 866-575-4791
Fax: +1 973-895-5376
E-mail: contact@amcbridge.com

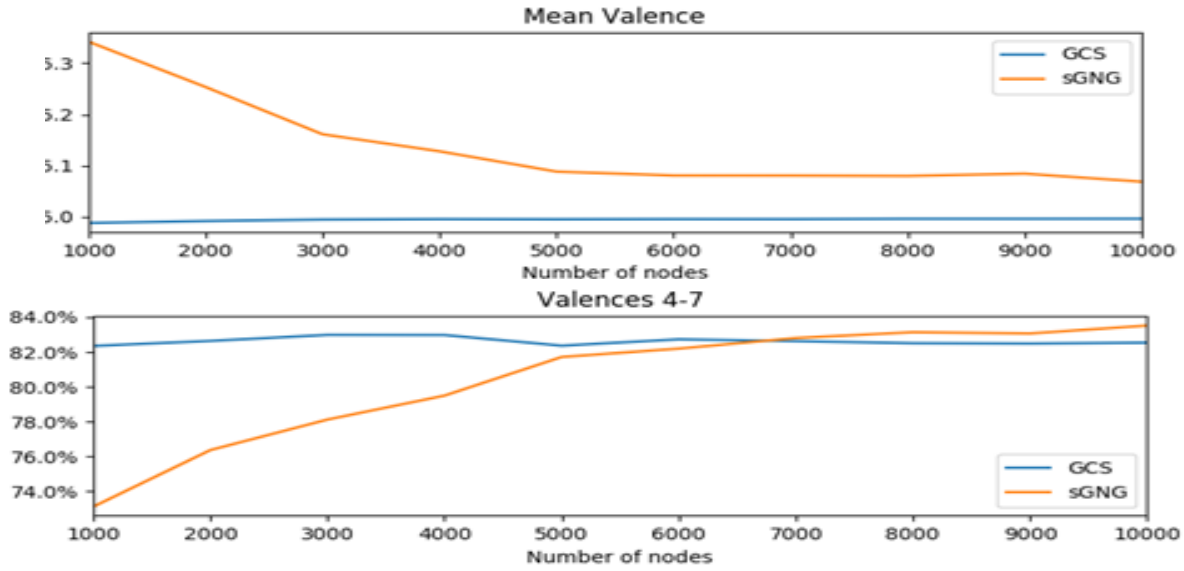

Figure 13. The mean valence and valences 4-7 metrics for algorithms on the Gear model.

Model: Arm

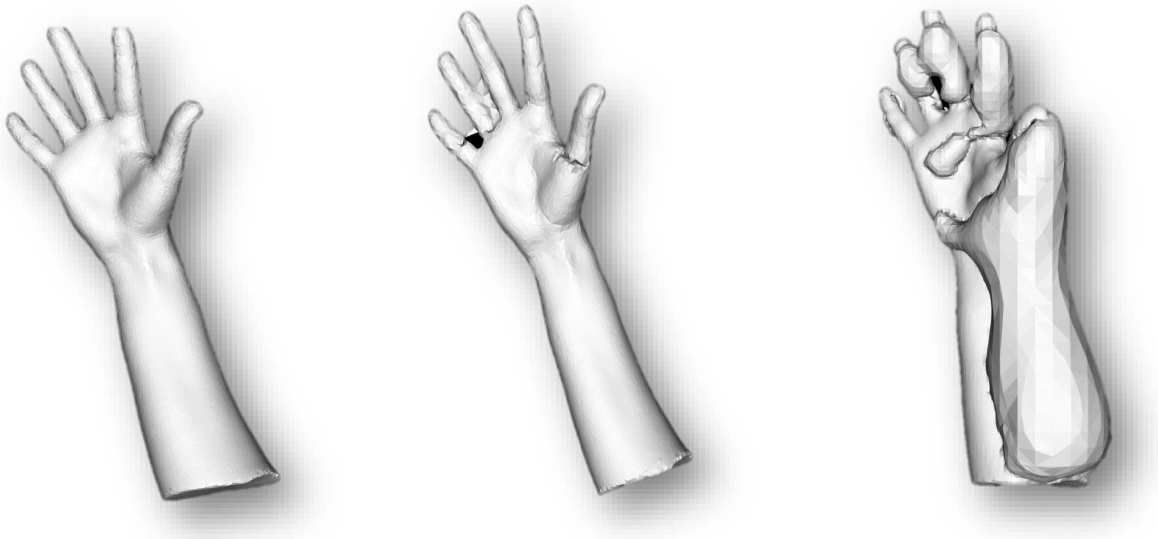

Figure 14. sGNG (left) reconstructed smooth arm surface, GCS (middle) produced arm with a few cuts and "webbed fingers". PCL Poisson algorithm (right) reconstructed arm with an unexpected part.

Tel: +1 866-575-4791
Fax: +1 973-895-5376
E-mail: contact@amcbridge.com

Model: Armadillo

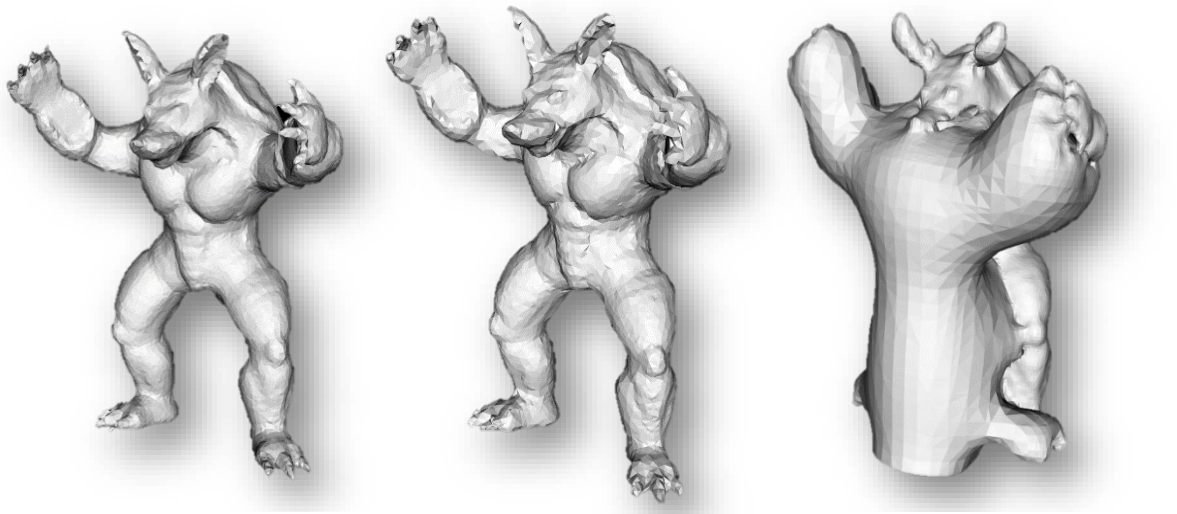

Figure 15. sGNG (left) and GCS (middle) reconstructed smooth and consistent body of the Armadillo. PCL Poisson reconstruction (right) has lots of errors.

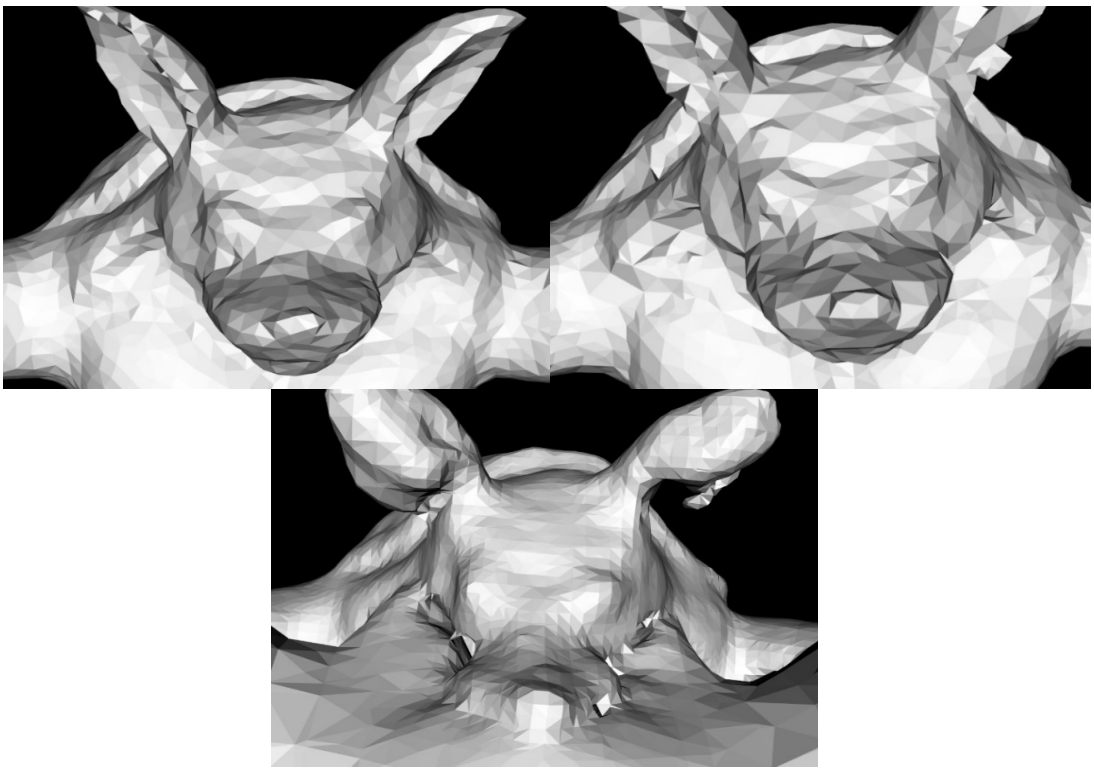

Figure 16. sGNG (top left) and GCS (top right) reconstructed Armadillo's face with the appropriate quality without any unexpected triangles and holes. PCL Poisson reconstruction (right) created a huge number of unexpected elements.

Tel: +1 866-575-4791
Fax: +1 973-895-5376
E-mail: contact@amcbridge.com

Statistics:

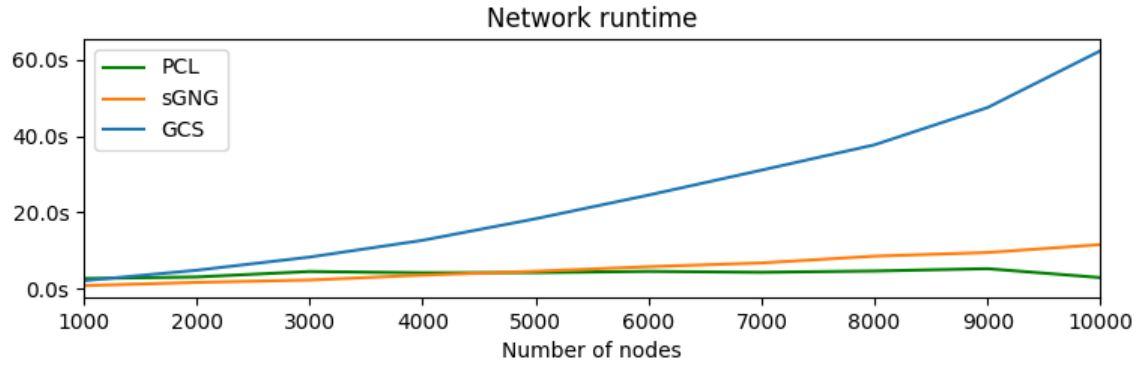

Figure 17. The performance test of reconstruction algorithms on the Armadillo model.

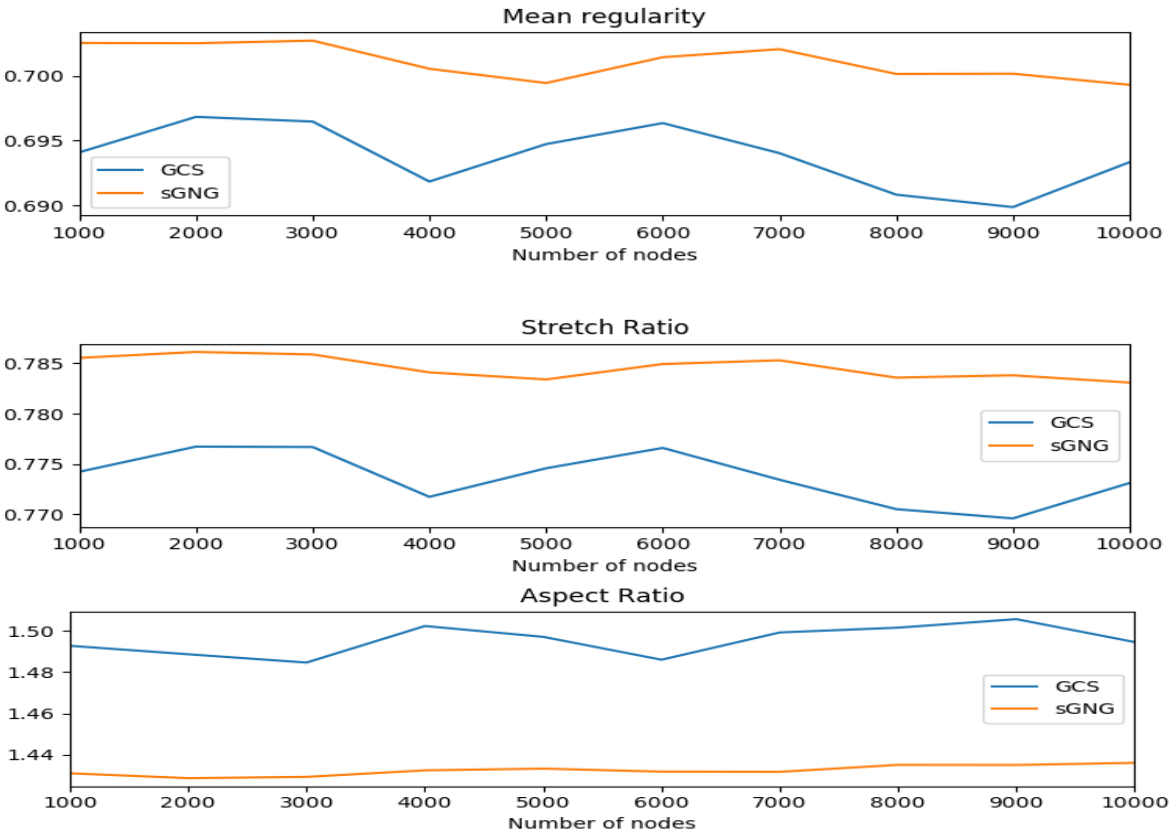

Figure 18. The mean valence and valences 4-7 metrics for algorithms on the Armadillo model.

Tel: +1 866-575-4791
Fax: +1 973-895-5376
E-mail: contact@amcbridge.com

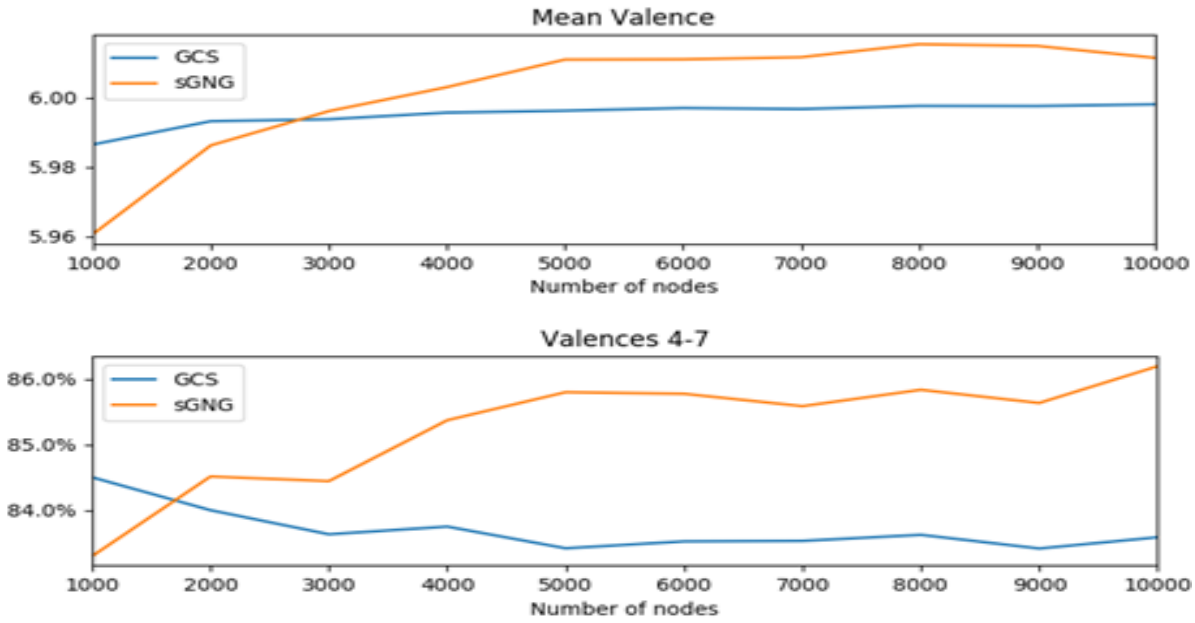

Figure 19. The mean regularity, aspect and stretch ration metrics for algorithms on the Armadillo model.

Evidently, sGNG algorithm provides better quality of reconstruction and works faster than GCS. However, Growing Cell Structures can assign the correct vertex normals for the reconstructed mesh, making the mesh suitable for calculating different descriptors. This could be important for modifying reconstructed models in such programs as MeshLab [22] in single Back-Face mode (Figure 20).

Figure 20. The MeshLab snapshot of sGNG (left) and GCS (right) reconstructions of the Armadillo model.

Tel: +1 866-575-4791
Fax: +1 973-895-5376
E-mail: contact@amcbridge.com

4. Multithreading Reconstruction Algorithm

The performance of the reconstruction process can be significantly improved by extending the reconstruction algorithm to multithreading.

The main idea of our multithreading algorithm is to partition the initial point cloud into boxes with an approximately equal number of points, reconstruct them separately and merge the resulting meshes (Figure 21). The cloud partition is performed by splitting the sub-point clouds with the overlapping along the specified axis recursively (Figure 22). This approach shows a significant quality improvement for the same runtime.

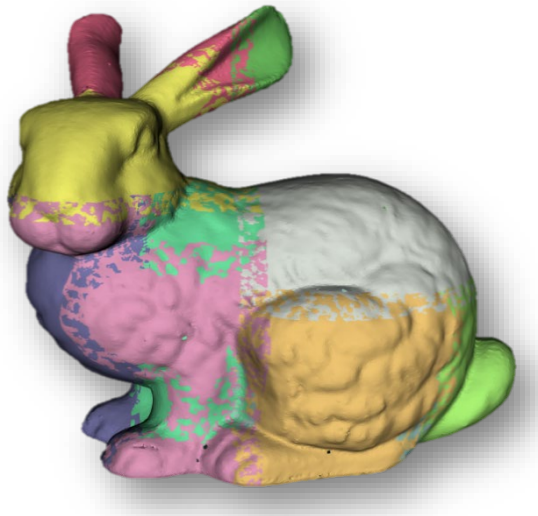

Figure 21. The reconstructed boxes are colored for better visualization.

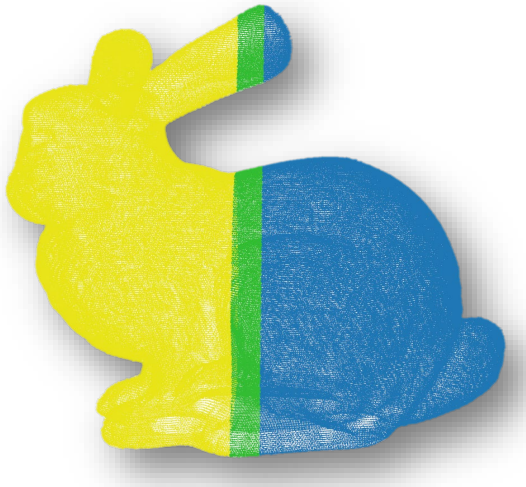

Figure 22. The partitioned point cloud. The partition with overlapping is performed.

Tel: +1 866-575-4791
Fax: +1 973-895-5376
E-mail: contact@amcbridge.com

Merging is performed recursively for overlapping box pairs concurrently. The merging algorithm is based on the adaptive mesh zippering [23] with the improvements for parallel planes. The main differences between the original algorithm and our modification is the choice of the add/remove thresholds and other mesh smoothing approach. The node add/remove thresholds are based on the average edge length and standard deviation, which provides the scalability of the algorithm. In addition, the iteration threshold has been added to protect the algorithm from an infinite loop due to the lack of points in the opposite mesh.

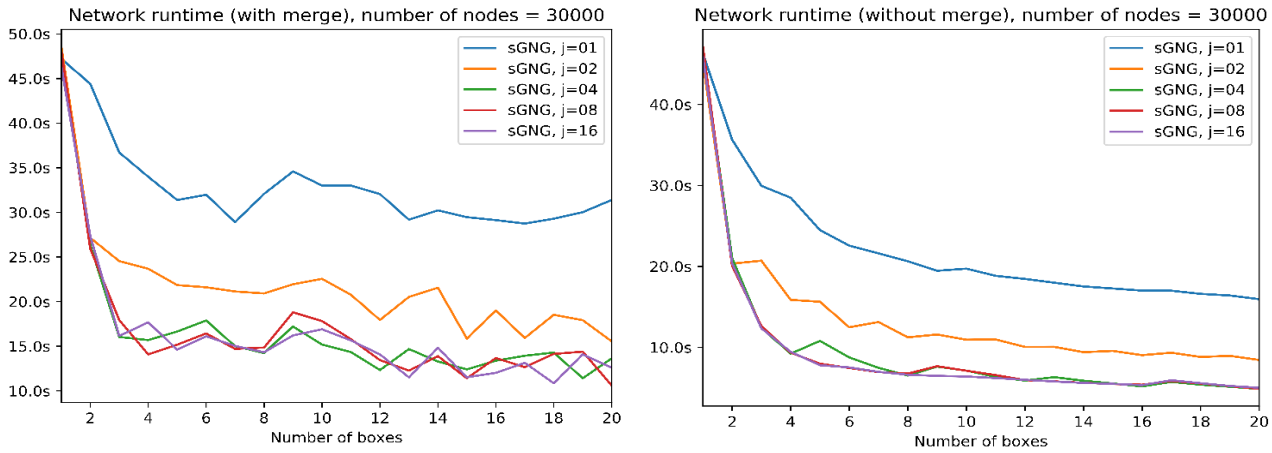

Figure 23. The performance test of sGNG reconstruction algorithm on Stanford Bunny model with different number of threads (jobs) and 30,000 resulting nodes (summary).

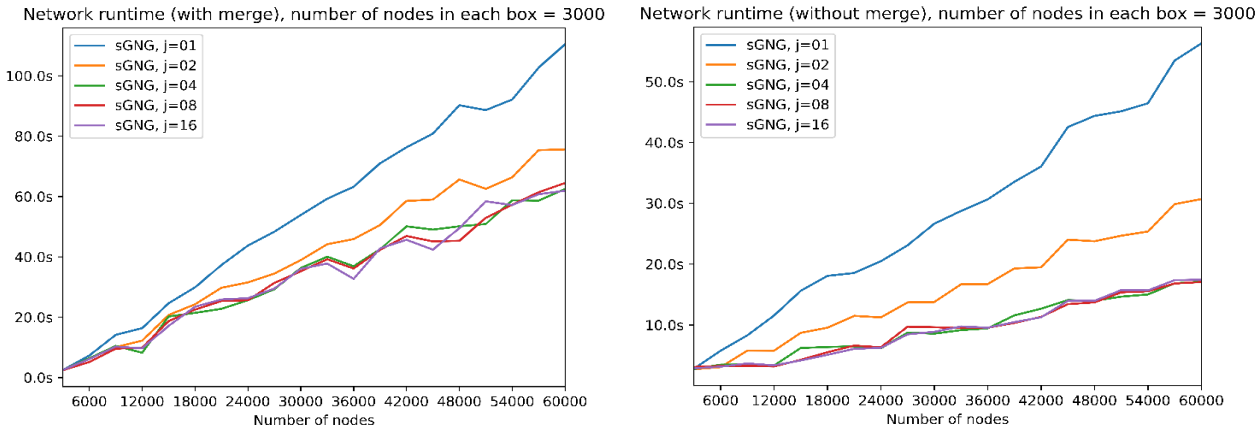

Figure 24. The performance test of sGNG reconstruction algorithm on Gear model with different number of threads (jobs) and 3,000 nodes in each box.

The original weighted Laplacian smoothing has been replaced with the Bilaplacian smoothing flow that preserves mesh features and is applied not to the bounding nodes, but to its non-bounding neighbors.

Tel: +1 866-575-4791
Fax: +1 973-895-5376
E-mail: contact@amcbridge.com

The analytics (Figures 23, 24) show that the multithreading algorithm with merging is about 3 times faster than the original one. All tests were performed on a system with Intel Core i5 3350P 3.10 GHz, 16 GB RAM. The number of threads supported by the computer is equal to 3. As we can see, the speed improvement is almost linear.

5. Multi-Processor Reconstruction Algorithm Based on MPI

The other way to improve performance of the reconstruction process is to use Message Passing Interface technology. We combined multithreading and MPI, to check out how it can improve reconstruction speed on large point clouds.

Table 1: MPI parameters.

Parameter type	Value
Number of nodes, used for MPI	3
Number of processes per node	1
Number of threads per process	varies from 2 to 12

Table 2: Computer specifications used for MPI.

Computer number	Options	Values
1	Processor:	Intel(R) Core(TM) i5-3350P CPU 3.10GHz
	RAM:	15.63
2	Processor:	Intel(R) Core(TM) i5-3350P CPU 3.10GHz
	RAM:	7.77
3	Processor:	Intel(R) Core(TM) i5-3350P CPU 3.10GHz
	RAM:	7.77

For the reconstruction we use two colored point clouds. You can see input and output results below.

Tel: +1 866-575-4791
Fax: +1 973-895-5376
E-mail: contact@amcbridge.com

Model: Truck. Number of points: 1,665,853.

Figure 25. The snapshot of the Truck model.

Output:

Figure 26. The MeshLab snapshot of sGNG reconstruction of the Truck model, nodes per box = 80,000, boxes = 10, with merge.

Tel: +1 866-575-4791
Fax: +1 973-895-5376
E-mail: contact@amcbridge.com

Cluster reconstruction analytics

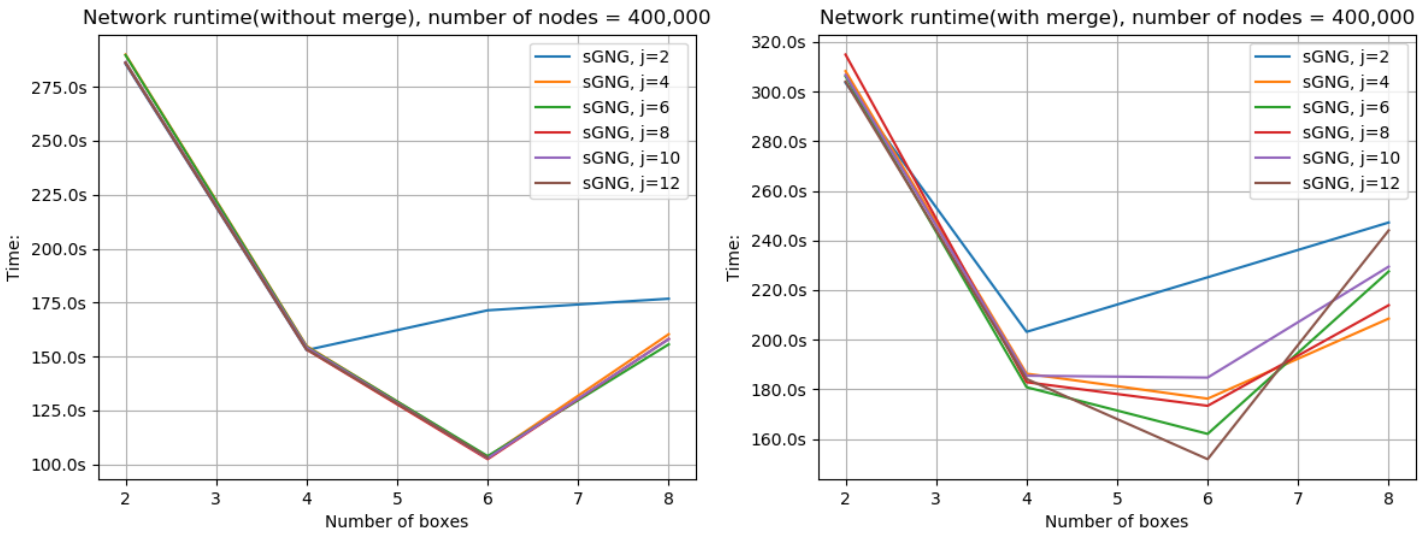

Figure 27. The performance test of sGNG reconstruction algorithm on Truck model with different numbers of threads (jobs) and 400,000 resulting nodes (summary).

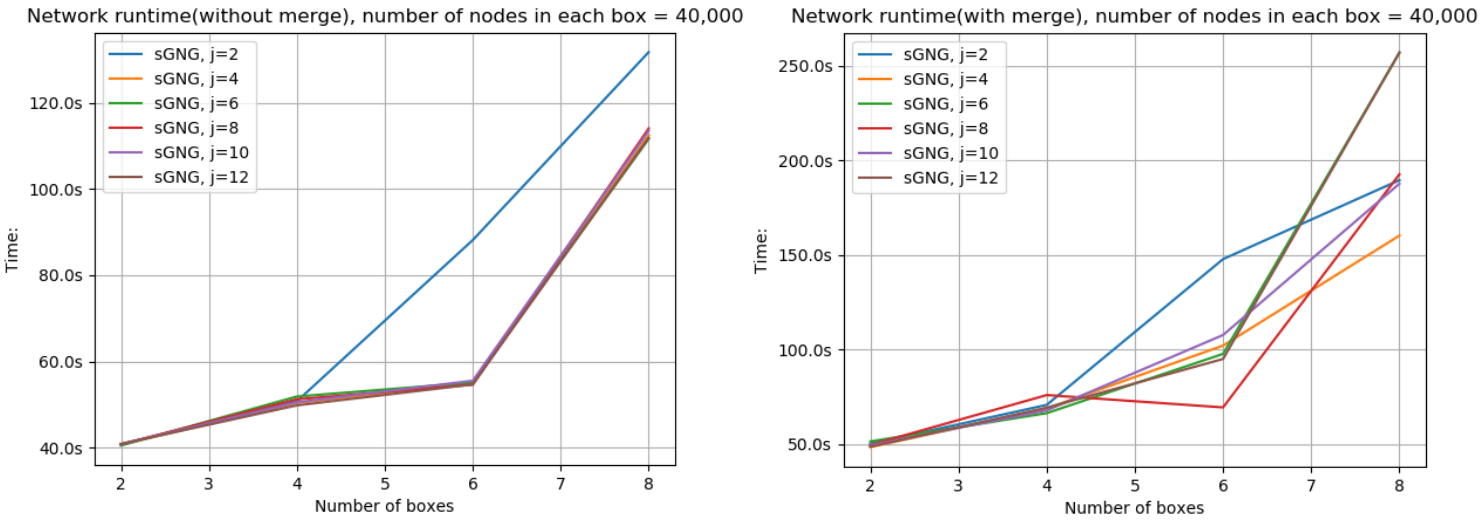

Figure 28. The performance test of sGNG reconstruction algorithm on Truck model with different numbers of threads (jobs) and 40,000 nodes in each box.

303 Wyman Street, Suite 300 Waltham, MA 02451, USA
www.amcbridge.com

Tel: +1 866-575-4791
Fax: +1 973-895-5376
E-mail: contact@amcbridge.com

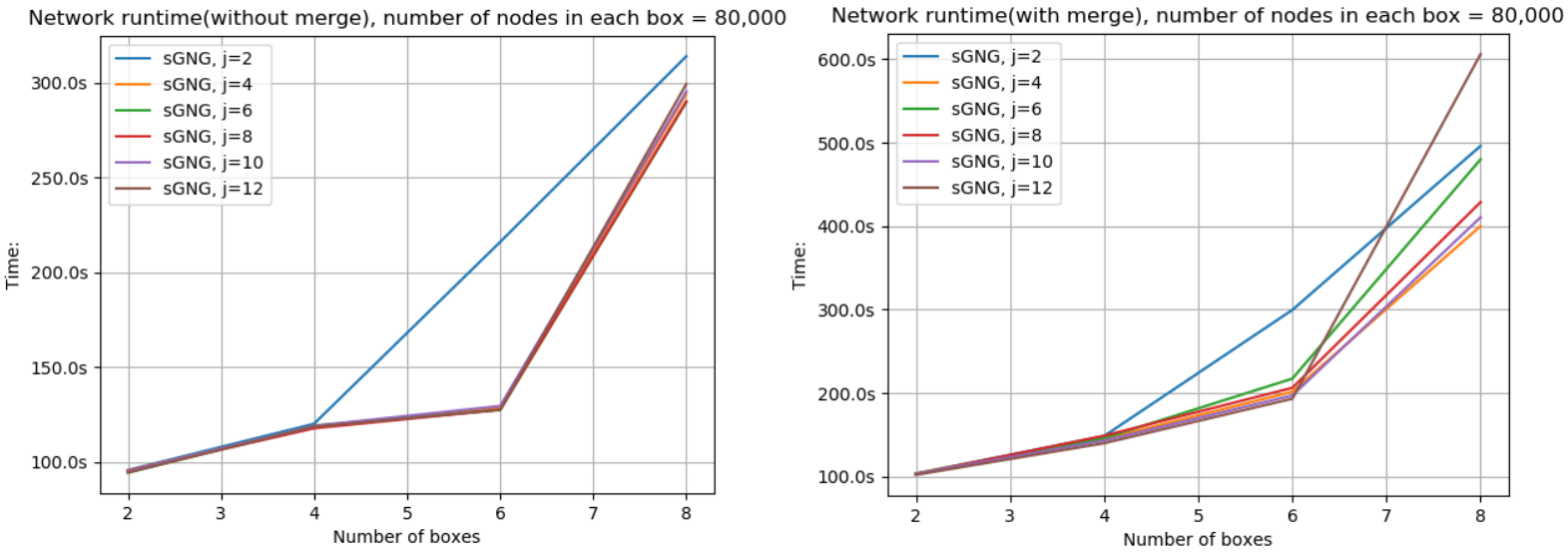

Figure 29. The performance test of sGNG reconstruction algorithm on Truck model with different numbers of threads (jobs) and 80,000 nodes in each box.

Single-computer reconstruction analytics

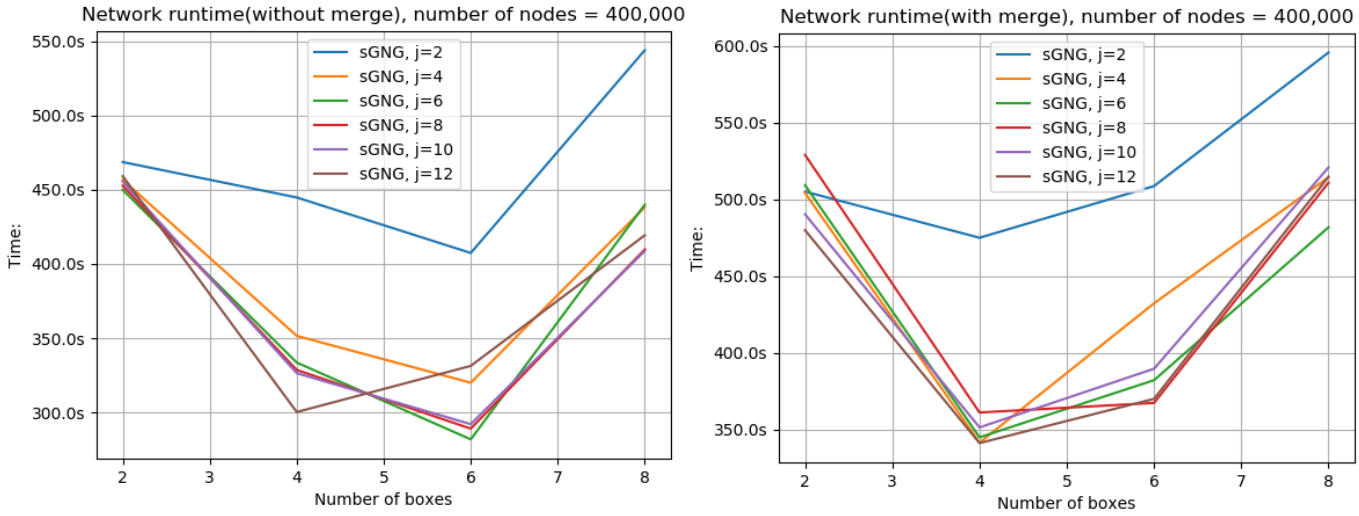

Figure 30. The performance test of sGNG reconstruction algorithm on Truck model with different numbers of threads (jobs) and 400,000 resulting nodes (summary).

Tel: +1 866-575-4791
Fax: +1 973-895-5376
E-mail: contact@amcbridge.com

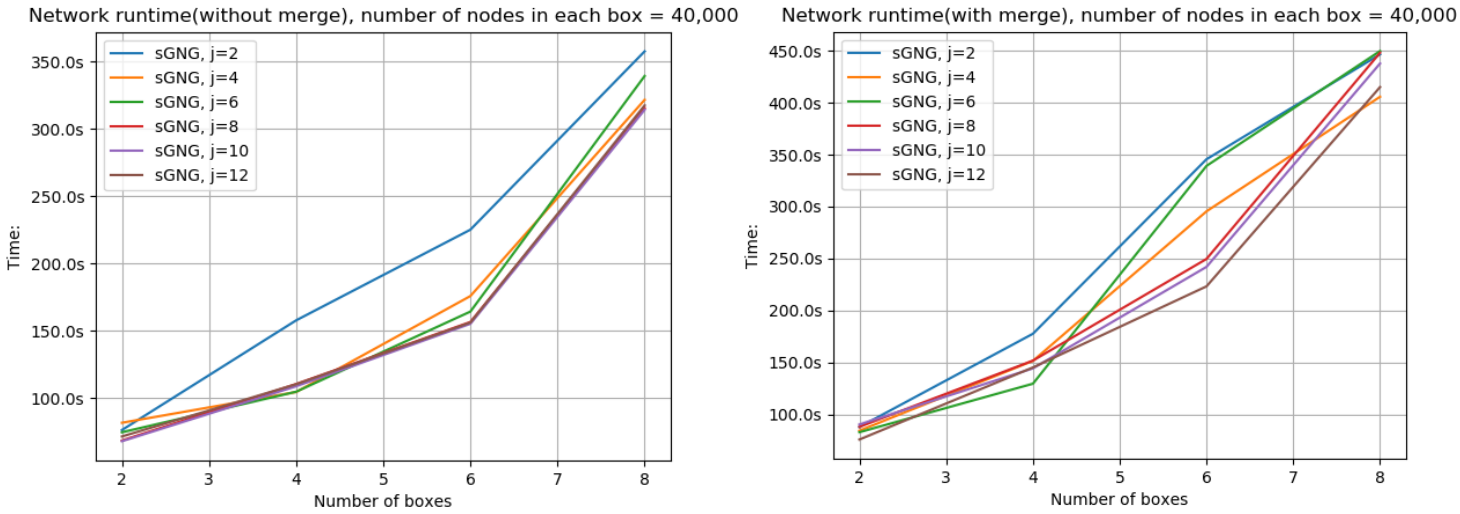

Figure 31. The performance test of sGNG reconstruction algorithm on Truck model with different numbers of threads (jobs) and 40,000 nodes in each box.

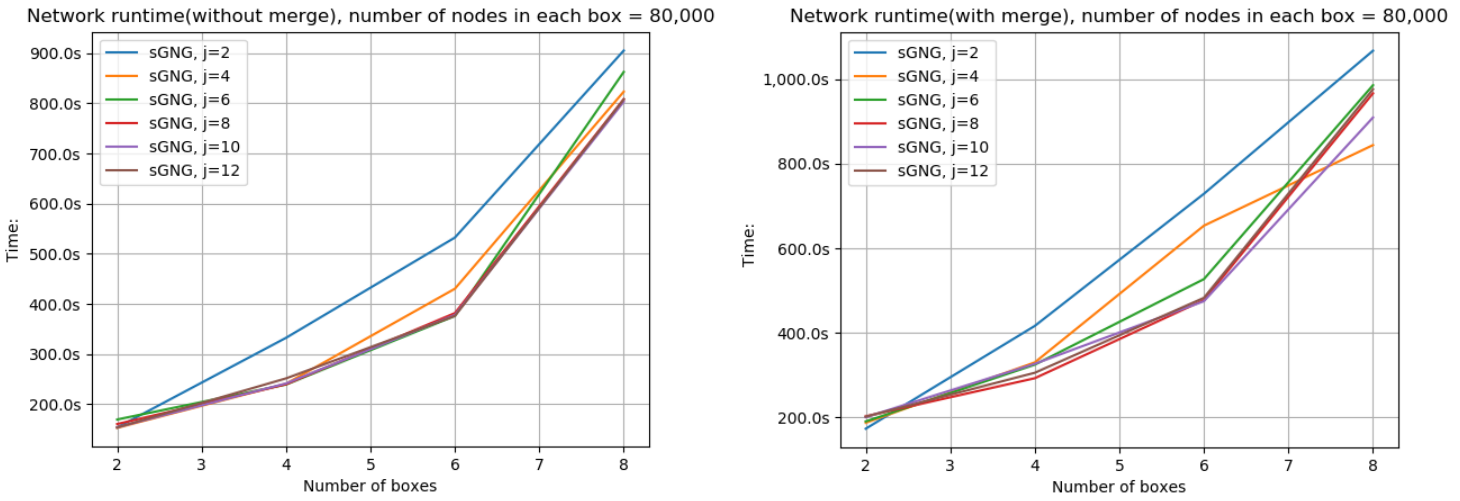

Figure 32. The performance test of sGNG reconstruction algorithm on Truck model with different numbers of threads (jobs) and 80,000 nodes in each box.

Tel: +1 866-575-4791
Fax: +1 973-895-5376
E-mail: contact@amcbridge.com

Model: Car. Number of points: 3,098,633.

Figure 33. The snapshot of the Car model.

Output:

Figure 34. The MeshLab snapshot of sGNG reconstruction of the Car model, nodes per box = 100,000, boxes = 8, with merge.

Tel: +1 866-575-4791
Fax: +1 973-895-5376
E-mail: contact@amcbridge.com

Cluster reconstruction analytics

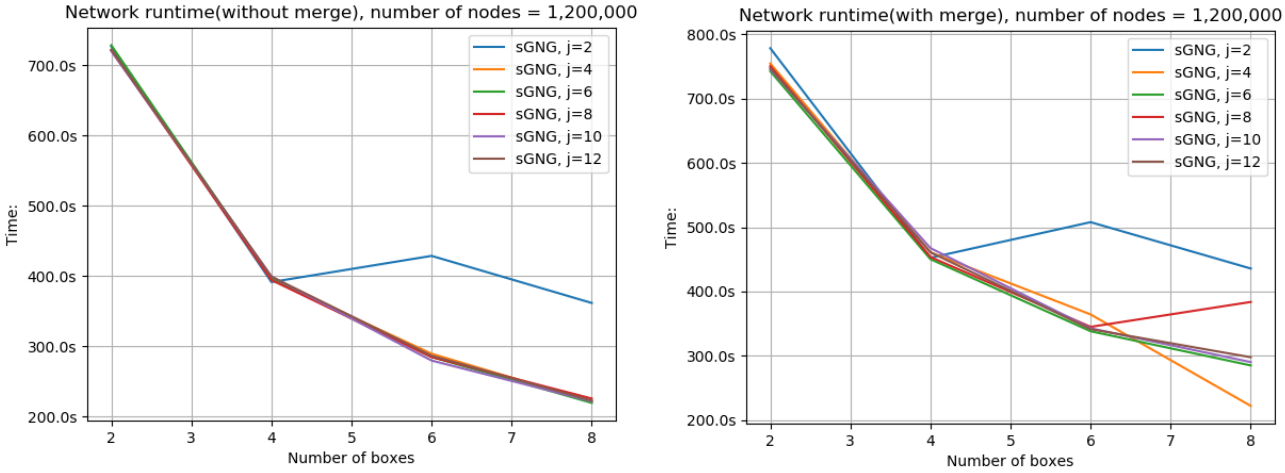

Figure 35. The performance test of sGNG reconstruction algorithm on Car model with different numbers of threads (jobs) and 1,200,000 resulting nodes (summary).

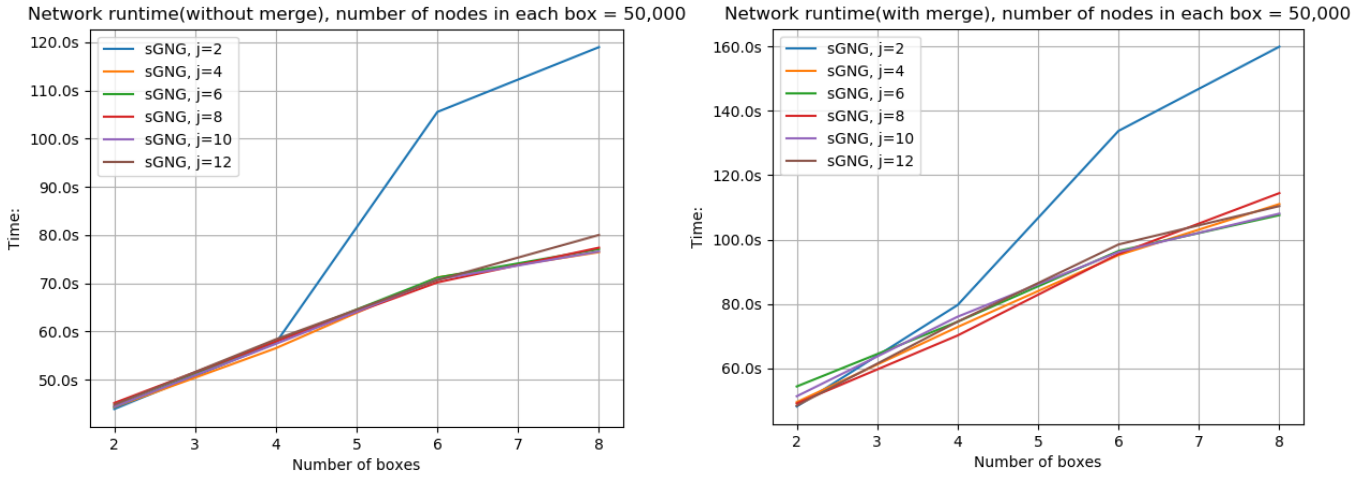

Figure 36. The performance test of sGNG reconstruction algorithm on Car model with different numbers of threads (jobs) and 50,000 nodes in each box.

Tel: +1 866-575-4791
Fax: +1 973-895-5376
E-mail: contact@amcbridge.com

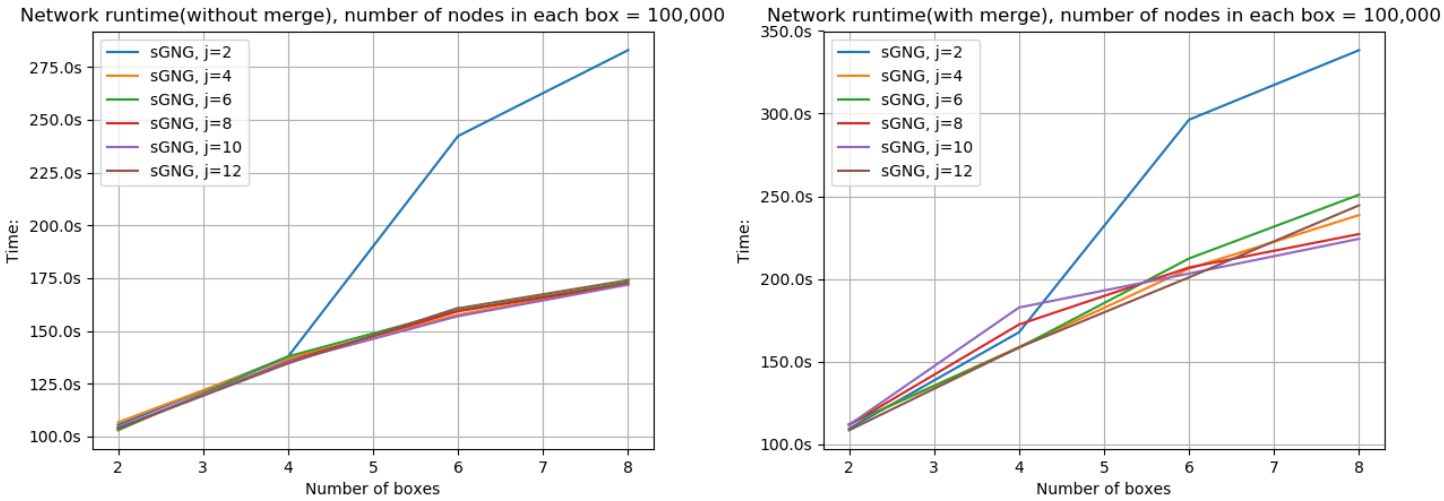

Figure 37. The performance test of sGNG reconstruction algorithm on Car model with different numbers of threads (jobs) and 100,000 nodes in each box.

Single-computer reconstruction analytics

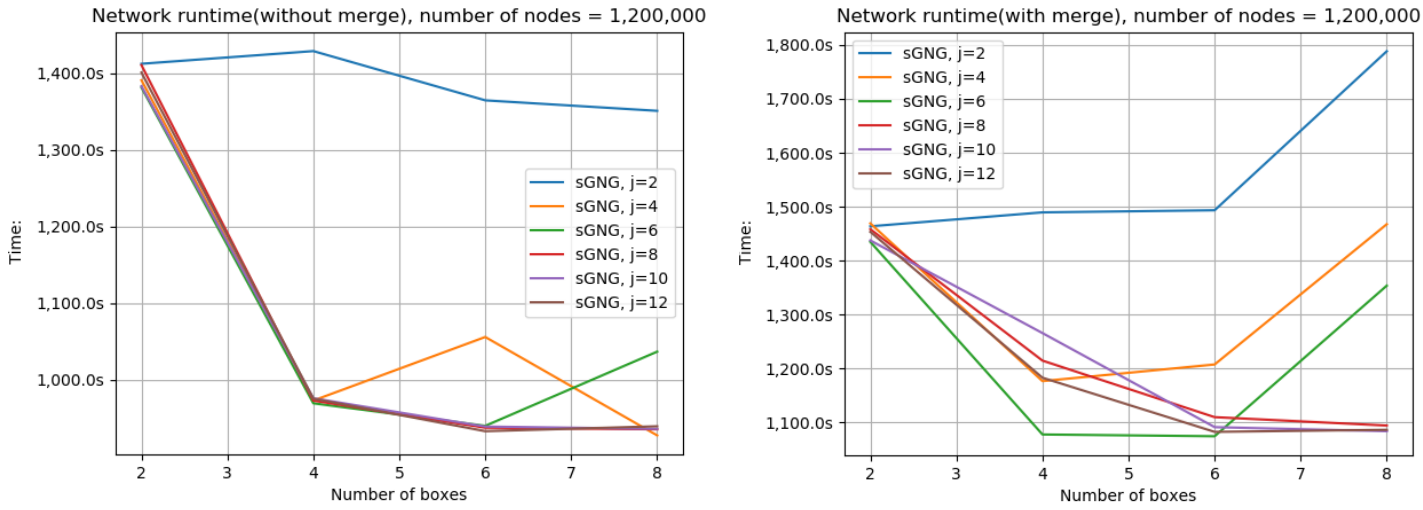

Figure 38. The performance test of sGNG reconstruction algorithm on Car model with different numbers of threads (jobs) and 1,200,000 resulting nodes (summary).

Tel: +1 866-575-4791
Fax: +1 973-895-5376
E-mail: contact@amcbridge.com

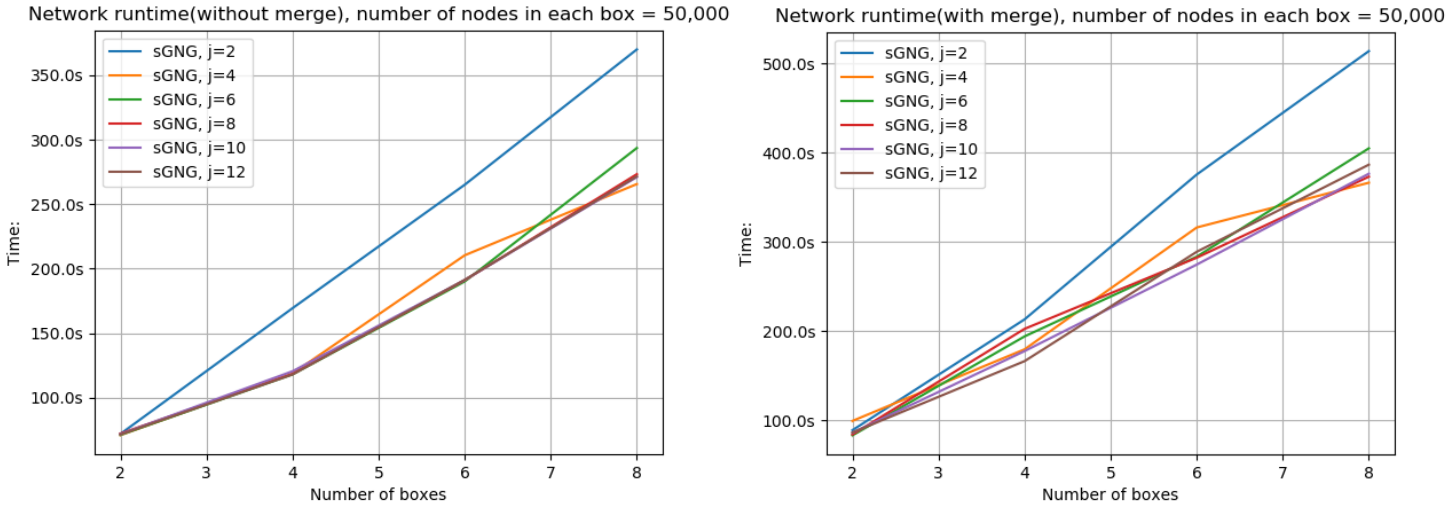

Figure 39. The performance test of sGNG reconstruction algorithm on Car model with different numbers of threads (jobs) and 50,000 nodes in each box

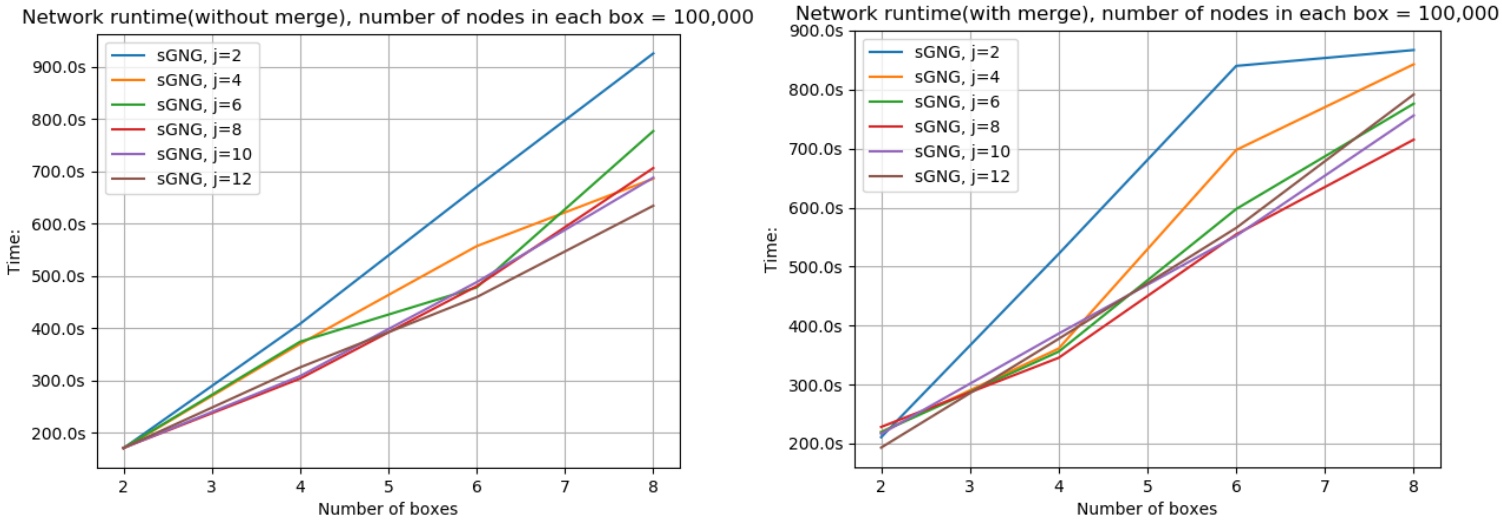

Figure 40. The performance test of sGNG reconstruction algorithm on Car model with different numbers of threads (jobs) and 100,000 nodes in each box.

The analytics (Figures 27-32, 35-40) shows that the multithreading reconstruction with MPI is about 2x faster with three nodes than the original one.

Tel: +1 866-575-4791
Fax: +1 973-895-5376
E-mail: contact@amcbridge.com

6. Further Directions

The quality of reconstructed mesh could be improved with combining both methods (sGNG and GCS) to reconstruct smooth mesh with the correct vertex normals.

The existing quality metrics could be augmented with visual quality metrics that could evaluate perceptional distortions introduced after point cloud reconstruction.

The reconstructed mesh could be used for further segmentation into meaningful parts (reconstruction of 3D scans of separate objects).

Tel: +1 866-575-4791
Fax: +1 973-895-5376
E-mail: contact@amcbridge.com

Conclusion

Table 3: The summary table of metrics values calculated for different meshes reconstructed by sGNG, GCS and PCL with the node number equal to 10,000, number of threads equal to 1, on system with Intel Core i5 3350P 3.10 GHz, 16 GB RAM.

Metric	Algorithm	Stanford Bunny	Gear	Arm	Armadillo
Performance (sec)	sGNG	12.76	13.05	9.45	11.02
	GCS	67.05	84.27	69.06	66.02
	PCL	3.04	2.73	2.66	2.59
Mean Valence	sGNG	6.004	6.070	6.00	6.01
	GCS	5.998	5.995	5.998	5.999
Valences 4-7 (%)	sGNG	86.81	83.81	86.09	86.17
	GCS	83.56	82.57	83.61	83.88
Mean Regularity	sGNG	0.696	0.664	0.693	0.699
	GCS	0.692	0.678	0.692	0.694
Aspect	sGNG	1.446	1.534	1.448	1.436
	GCS	1.501	1.532	1.498	1.495
Stretch	sGNG	0.779	0.747	0.777	0.783
	GCS	0.771	0.758	0.772	0.774

Table 4: The table of metrics values calculated for different meshes reconstructed by sGNG, with the node number equal to 10,000, number of threads on each computer equal to 4, number of boxes equal to 1, with MPI.

Metric	Algorithm	Stanford Bunny	Gear	Arm	Armadillo
Performance (sec)	sGNG	4.440	4.918	3.532	4.370

The research demonstrates that Self-Organizing Maps are suitable for 3D Surface Reconstruction. The testing shows that GCS approach provides comparable results only on meshes that are not difficult, while the sGNG approach reconstructs meshes with a huge number of small details very well. The sGNG approach is advisable to use for reconstruction in most cases when the vertex normals are unimportant. The GCS showed inferior

Tel: +1 866-575-4791
Fax: +1 973-895-5376
E-mail: contact@amcbridge.com

results but it could be useful for reconstruction of meshes with the correct vertex normals for further processing. PCL Poisson algorithm works faster, but the quality of reconstruction is unsuitable, so it could be used only for previewing of the target mesh.

About AMC Bridge

AMC Bridge is a trusted software technology partner for engineering, manufacturing, and construction enterprises, whether they are actively pursuing AI-driven digital transformation or only beginning to recognize its potential. We help organizations achieve real ROI in production, not in demos, by delivering production-ready software and end-to-end solutions for the transformation journey.

We design, build, and integrate enterprise-grade software – applications, workflow extensions for CAD/PLM/BIM, data integrations, and AI-enabled features – and deploy them with monitoring and lifecycle management so they remain reliable over time. Our services include assessing data readiness; preparing and unifying product and project data; and embedding AI into the workflows teams use every day. With 25+ years of industrial software expertise and deep ecosystem partnerships, including Aras, Autodesk, Bentley, Dassault Systèmes, PTC, Siemens, Tech Soft 3D, and others, we empower enterprises to move confidently from experimentation to operational AI at scale. For more information, visit amcbridge.com.

References

[1] A. Ng, *Machine Learning.*

[2] A. D. M. B. Junior, A. A. D. D. Neto and D. a. D. J. Melo, "A self-organized neural network for 3D surface reconstruction".

[3] P. Jenke, M. Wand, M. Bokeloh, A. Schilling and W. Straßer, "Bayesian point cloud reconstruction," in *Computer Graphics Forum*, 2006.

[4] H. Hoppe, "Poisson surface reconstruction and its applications," in *Proceedings of the 2008 ACM symposium on Solid and physical modeling*, 2008.

[5] T. Kohonen, "The self-organizing map," *Neurocomputing,* vol. 21, pp. 1-6, 1998.

[6] T. Vierjahn, N. Henrich, K. H. Hinrichs and S. Mostafawy, "sGNG: Online Surface Reconstruction based on Growing Neural Gas," Germany, 2013.

[7] I. V. Ivrissimtzis, W.-K. Jeong and H.-P. Seidel, "Using growing cell structures for surface reconstruction," in *Shape Modeling International, 2003*, 2003.

Tel: +1 866-575-4791
Fax: +1 973-895-5376
E-mail: contact@amcbridge.com

[8] Wikipedia, *Polygon mesh --- Wikipedia, The Free Encyclopedia,* 2017.

[9] M. Caudill, "Neural Networks Primer, Part I," *AI Expert,* vol. 2, pp. 46-52, December 1987.

[10] B. Fritzke and others, "A growing neural gas network learns topologies," *Advances in neural information processing systems,* vol. 7, pp. 625-632, 1995.

[11] B. Fritzke, "Growing cell structures—a self-organizing network for unsupervised and supervised learning," *Neural networks,* vol. 7, pp. 1441-1460, 1994.

[12] C. A. T. Mendes, M. Gattass and H. Lopes, "FGNG: A Fast Multi-dimensional Growing Neural Gas Implementation," *Neurocomput.,* vol. 128, pp. 328-340, March 2014.

[13] I.P. Ivrissimtzis, W-K. Jeong H-P. Seidel," Using Growing Cell Structures for Surface Reconstruction", Germany

[14] M. Goelke, *Element Quality and Checks – Intro,* 2014.

[15] S. Orts, J. Garcia-Rodriguez, D. Viejo, M. Cazorla and V. Morell, "GPGPU implementation of growing neural gas: Application to 3D scene reconstruction," *Journal of Parallel and Distributed Computing,* vol. 72, pp. 1361-1372, 2012.

[16] C. A. T. Mendes, M. Gattass and H. Lopes, "FGNG: A fast multi-dimensional growing neural gas implementation," *Neurocomputing,* vol. 128, pp. 328-340, 2014.

[17] D. Fišer, J. Faigl and M. Kulich, "Growing neural gas efficiently," *Neurocomputing,* vol. 104, pp. 72-82, 2013.

[18] R. B. Rusu and S. Cousins, "3D is here: Point Cloud Library (PCL)," in *{IEEE International Conference on Robotics and Automation (ICRA)}*, Shanghai, 2011.

[19] W. Schroeder, K. Martin and B. Lorensen, The Visualization Toolkit: An Object-oriented Approach to 3D Graphics, Kitware, 2006.

[20] J. D. Hunter, "Matplotlib: A 2D graphics environment," *Computing In Science \& Engineering,* vol. 9, pp. 90-95, 2007.

[21] B. Fritzke, *Growing Cell Structures,* 1997.

[22] P. Cignoni, M. Callieri, M. Corsini, M. Dellepiane, F. Ganovelli and G. Ranzuglia, "MeshLab: an Open-Source Mesh Processing Tool," in *Eurographics Italian Chapter Conference*, 2008.

[23] R. Schmidta and T. Brochua, "Adaptive Mesh Booleans".